




Anomalous Transition in Thermal Conductivity in Germanene Monolayer

Sapta Sindhu Paul Chowdhury , Sourav Thapliyal , and Santosh Mogurampelly 

*Department of Physics, Indian Institute of Technology Jodhpur
N.H. 62, Nagaur Road, Karwar, Jodhpur, Rajasthan, India - 342030.*

(Dated: November 22, 2024)

We report an anomalous temperature-induced transition in thermal conductivity in germanene monolayer around a critical temperature $T_c = 350$ K. Equilibrium molecular dynamics simulations reveal a transition from $\kappa \sim T^{-2}$ scaling below T_c to $\kappa \sim T^{-1/2}$ above, contrasting with conventional $\kappa \sim T^{-1}$ behavior. This anomalous scaling correlates with long-scale characteristics timescale τ_2 obtained from double exponential fitting of heat current autocorrelation function. Phonon mode analysis using normal mode decomposition indicates that a redshift in TA phonons reduces the acoustic-optical phonon gap, enhancing the phonon-phonon scattering and driving the anomalous scaling behavior. Moreover, non equilibrium simulations find a convergent thermal conductivity of germanene with sample size, in agreement with mode coupling theory, owing to high scattering of ZA phonons due to the inherent buckling of germanene.

I. INTRODUCTION

Germanene, the two-dimensional (2D) analog of germanium, is an experimentally realized distinctive 2D material with promising electronic and thermal properties [1, 2]. Composed of a single atomic layer of Ge atoms in a hexagonal lattice [3], germanene differs fundamentally from planar 2D materials like graphene, h-BN etc., due to its intrinsic buckling which introduces out-of-plane atomic displacements [4]. This inherent buckling not only enables tunable properties [5] as a result of additional degrees of freedom but also enhances scattering of out-of-plane (flexural) phonons, a feature with significant implications for germanene's thermal transport behavior.

Several studies have focused on understanding the electronic properties of germanene [6]. The electrical and thermal conductivity have been previously studied by Chegel et al. [7]. It is found that the band gap of germanene can be opened and increased to 20-310 meV [8]. Application of germanene is explored in case of Li and Na ion batteries resulting in high charge capacities [9]. Electronic properties due to external defects are found to be highly sensitive with vanishing Dirac cone [10]. Similarly, functionalization with H, I, F, Cl and Br is proposed for topological insulating device based on germanene [11].

The thermal transport of germanene is reported in a few works, compared to the extensive studies based on electronic properties. Previous work on the thermal properties of germanene reports a low thermal conductivity, attributed to its intrinsic buckling and relatively high atomic mass. Peng et al. [12] reported a thermal conductivity of 2.4 W/(m K) at 300 K using the Boltzmann transport equation with *ab-initio* force constants, while Das et al. [13] found 3.1 W/(m K) using the Debye-Callaway model. These values contrast sharply with planar 2D materials, supporting the hypothesis that

buckling reduces thermal transport efficiency [14]. External strain, however, significantly enhances thermal conductivity, with pronounced size effects under increased strain [15]. Silicene-germanene superlattices also show a non-monotonic thermal conductivity due to phonon confinement effects [16]. Vibrational studies indicate that specific heat in germanene follows a T^2 dependency at low temperatures, further highlighting its unique thermal characteristics [17].

While the thermal transport properties of graphene have been extensively studied [18–20], systematic investigations into buckled monolayer germanene are limited. An in-depth understanding of phonon propagation and thermal conductivity in such 2D materials is crucial for their optimization in high-performance applications. To date, however, the literature lacks comprehensive experimental data and theoretical analyses on thermal transport in germanene, particularly on the role of temperature induced phonon relaxation effects. This study seeks to fill this gap, presenting detailed analyses of germanene's temperature-dependent phonon thermal transport and its implications for future applications.

This paper is organized as follows: Sec. II provides an overview of the theoretical framework and computational methodology. In Sec. III, we present our findings: Sec. IIIA discusses the temperature-dependent structural behavior of germanene, followed by thermal conductivity calculations and their temperature dependence in Sec. IIIB. Sec. IIIC explores the mechanisms underlying phonon thermal transport, with a detailed analysis of phonon dispersion and linewidth, and their temperature dependence. Sec. IIID examines the influence of sample size on thermal conductivity. Finally, Sec. IV summarizes the key findings and their implications.

II. COMPUTATIONAL DETAILS

We use the Large-scale Atomic/Molecular Massively Parallel Simulator (Lammps) [21] for carrying out the molecular dynamics simulations. The verlet algorithm

* santosh@iitj.ac.in

is used for integrating Newton's equation of motion. The modified Stillinger-Weber (SW) potential is used for modeling the interatomic interactions. We take the optimized parameters of SW potential for all the simulations from the work of Jiang et al [22]. It is noteworthy that the among available choices of potentials, Tersoff potential is unsuitable for our calculations as the sheets deform at 700 K [23]. The periodic boundary condition has been applied in all three directions. However, to make the out-of-plane direction of germanene monolayer aperiodic, we have added 50 Å vacuum in the Z-direction. To obtain optimized geometry molecular mechanics based minimization with steepest descent and conjugate gradient are carried out with a tolerance of 10^{-14} for energy and 10^{-14} eV/Å for force. It is noteworthy that bond order Tersoff potential leads to unstable geometry at the high temperature regime, so SW potential must be chosen to simulate the systems [23]. To equilibrate the systems for thermal conductivity calculations, we have simulated the system in isothermal-isobaric (NPT) ensemble and thereafter in isothermal (NVT) ensemble for 1 ns respectively (Fig. S1, S2 in SI) with 1 fs timestep for integrating Newton's equation of motion. We use the Nose-Hoover thermostat with coupling constant of 0.1 ps and Nose-Hoover barostat with 1 ps coupling constant for maintaining temperature (100-950 K) and pressure (0 bar) throughout simulation runs. We calculate the thermal conductivity by ensemble averaging 30 independent trajectories, created by randomizing the velocity distribution of Ge atoms. Each trajectory is simulated for an 2 ns with fine timestep of 0.1 fs in NVT ensemble (Fig. S3 in SI).

In equilibrium formalism, the thermal conductivity (κ) at a ambient temperature T is calculated by using Green-Kubo relation by integrating the heat current auto-correlation function:

$$\kappa(T) = \frac{1}{Vk_B T^2} \int_0^\infty \langle \mathbf{S}(0) \cdot \mathbf{S}(t) \rangle dt. \quad (1)$$

Here, the volume is calculated as $V=L_x \times L_y \times 4.24$, where L_x and L_y are the dimension of the simulation cell in X and Y direction and the van der Waals radius of Ge atoms is taken as the thickness. The heat current operator, $\mathbf{S}(t)$ is calculated by:

$$\mathbf{S}(t) = \sum_i E_i v_i + \frac{1}{2} \sum_{i < j} (f_{ij} \cdot (v_i + v_j)) r_{ij}, \quad (2)$$

with the force between i^{th} and j^{th} atom given by f_{ij} , E_i is the energy, v_i is the velocity of i^{th} atom and r_{ij} is the corresponding displacement vector. More details on the calculations of phonon density of state (PDOS), dispersion relation are available in our previous works [24, 25].

We use the Fourier's law to calculate the thermal conductivity from the non-equilibrium simulations, given by:

$$J = -\kappa \nabla T, \quad (3)$$

where J is the heatflux flowing from hotter to colder regions of the simulation. Unlike in case of equilibrium simulations, for simulating the systems in non equilibrium condition, we fix one end of the sheet to a higher temperature of 320 K and the other end of the system at 280 K by using Langevin thermostat, as implemented in Lammmps.

The phonon power spectrum is calculated from the velocity auto-correlation function by [26]:

$$G_{\mathbf{q}j}(\omega) = 2 \int_{-\infty}^{\infty} \langle v_{\mathbf{q}j}^*(0) v_{\mathbf{q}j}(\tau) \rangle e^{i\omega\tau} d\tau, \quad (4)$$

where, the velocity autocorrelation function is:

$$\langle v_{\mathbf{q}j}^*(0) v_{\mathbf{q}j}(\tau) \rangle = \lim_{t' \rightarrow \infty} \frac{1}{t'} \int_0^{t'} v_{\mathbf{q}j}^*(t + \tau) v_{\mathbf{q}j}(t) dt. \quad (5)$$

Here, $v_{\mathbf{q}j}$ is the velocity of phonon branch j corresponding to a wavevector \mathbf{q} , obtained from MD simulations. We use the normal mode decomposition technique to project atomic velocities on the wavevector \mathbf{q} :

$$\mathbf{v}_l^{\mathbf{q}}(t) = \sqrt{\frac{m_l}{N}} \sum_k e^{-i\mathbf{q} \cdot \mathbf{r}_{kl}^0} \mathbf{v}_{kl}(t). \quad (6)$$

Projecting into phonon eigenvector $\mathbf{e}(\mathbf{q}, j)$, we have:

$$v_{\mathbf{q}j}(t) = \sum_l \mathbf{v}_l^{\mathbf{q}}(t) \cdot \mathbf{e}_l^*(\mathbf{q}, j). \quad (7)$$

Now, the power spectrum is fitted with a Lorentzian to obtain the phonon linewidth $\gamma_{\mathbf{q}j}$ as:

$$G_{\mathbf{q}j} \equiv \frac{\langle |v_{\mathbf{q}j}(t)|^2 \rangle}{\frac{1}{2} \gamma_{\mathbf{q}j} \pi \left(1 + \left(\frac{\omega - \tilde{\omega}_{\mathbf{q}j}}{\frac{1}{2} \gamma_{\mathbf{q}j}} \right)^2 \right)}. \quad (8)$$

Here, ω is the frequency at peak, and γ represent the half width at half maximum. The phonon lifetime is calculated by $\tau = 1/(2\gamma)$.

III. RESULTS AND DISCUSSION

A. Effect of Temperature on Structural Geometry

Germanene, comprising a hexagonal lattice of Ge atoms, exhibits intrinsic buckling that distinguishes it from planar 2D materials like graphene and h-BN. All structural parameters are based on the experimentally reported geometry [27]. Molecular mechanics optimization yields a lattice constant of $a = 3.98$ Å and a buckling height of 0.71 Å, with the system maintaining the symmetry operations of the P-3m1 space group. A $32 \times 32 \times 1$ supercell containing 2048 Ge atoms is used for all simulations.

To investigate the thermal effects on the lattice geometry, we conduct simulations at a fixed pressure of 0

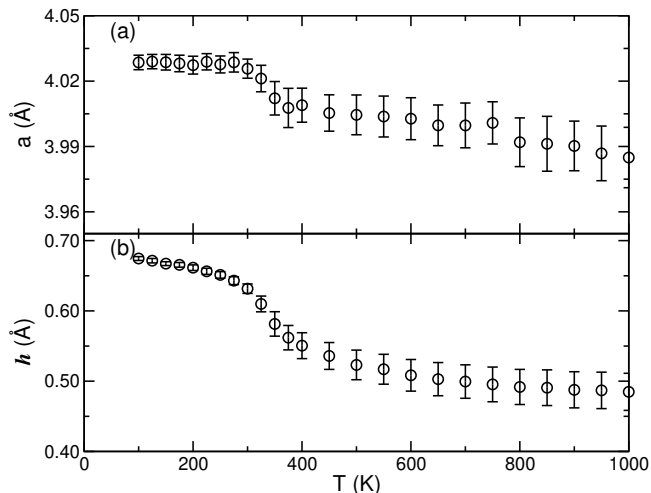


FIG. 1. (a) The lattice constant and (b) buckling height of a germanene monolayer as functions of temperature. Both lattice constant and buckling height decrease monotonically, with a rapid decline observed between 300 K and 400 K.

bar in NPT ensemble across a range of temperatures. Figure 1 (a,b) illustrates the temperature dependence of the lattice constant and buckling height. We observe a monotonic decrease in both parameters with increasing temperature, though their rates of change vary across different temperature regimes. At lower temperatures, the lattice constant remains nearly constant, while buckling height decreases. In the intermediate range (300-400 K), both lattice constant and buckling height show a more rapid decline at comparable rates. Beyond 400 K, however, the lattice constant stabilizes, while the buckling height continues to decrease at a slightly faster rate.

This temperature-dependent behavior reflects a dual mechanism of structural relaxation. Initially, as thermal energy increases, germanene primarily relaxes through reductions in buckling height, which equilibrate internal stresses without significantly altering the in-plane lattice. Around 300 K, further temperature increases lead to a cooperative relaxation between lattice constant contraction and buckling height reduction. As temperature increases beyond 400 K, the competing relaxations stabilize, with the lattice constant decreasing at a slower rate, and buckling remaining the dominant mode of structural adaptation.

B. Anomalous Transition in Thermal Conductivity

The thermal conductivity of a germanene monolayer is determined using equilibrium molecular dynamics simulations, yielding a value of 3.6 ± 0.4 W/m.K at room temperature, in close agreement with prior studies [12, 13, 23]. As illustrated in Figure 2, κ demonstrates a clear, monotonic decline with increasing temperature, typical of enhanced phonon-phonon scattering that limits heat

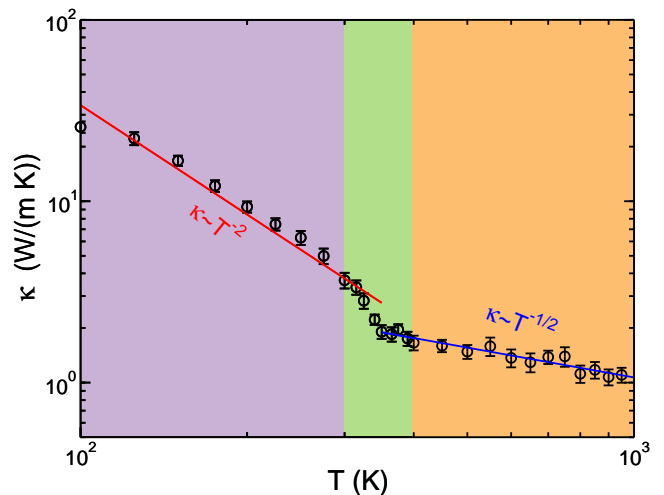


FIG. 2. Thermal conductivity of a germanene monolayer as a function of temperature. An anomalous transition in κ is observed near $T_c \sim 350$ K, with distinct power-law relations with exponents -2 and $-1/2$ below and above T_c , respectively.

transport at higher temperatures. However, a distinct and unexpected transition in thermal conductivity behavior occurs at a critical temperature $T_c \approx 350$ K, where the temperature scaling of κ markedly shifts, revealing unique thermal transport characteristics in germanene not observed in most 2D materials.

This transition is quantified by power-law fits to the data below and above T_c , showing that $\kappa \sim T^{-2}$ for temperatures below T_c and $\kappa \sim T^{-1/2}$ for temperatures above T_c . Such behavior deviates from the conventional $\kappa \sim T^{-1}$ trend typical for crystalline 2D systems, [28, 29] where phonon scattering rates are expected to yield a single scaling regime. The observed T^{-2} scaling below T_c indicates an unusually rapid decay in thermal conductivity with temperature, suggesting that lower-temperature heat transport in germanene is highly sensitive to the interactions between specific phonon modes, while higher temperatures favor a reduced sensitivity, as evidenced by the more gradual $T^{-1/2}$ scaling above T_c .

The observed shift from T^{-2} to $T^{-1/2}$ scaling at T_c highlights a critical threshold in the thermal behavior of germanene, demarcating two distinct heat transport regimes. Below T_c , enhanced thermal resistivity dominates due to specific phonon scattering interactions, while above T_c , these processes diminish or reconfigure, leading to a more stable thermal regime. This anomalous transition is likely tied to the unique buckled structure of germanene, offering key insights into designing germanene-based devices. In the following, we explore these mechanisms by analyzing the relaxation phenomena and phonon dispersion, density of states, and linewidths.

C. Mechanisms Underlying Phonon Thermal Transport

To investigate the underlying heat transport mechanisms in germanene, we analyze the nature of heat current autocorrelation function (HCACF) through double-exponential fitting:

$$\frac{\langle \mathbf{S}(0) \cdot \mathbf{S}(t) \rangle}{\langle \mathbf{S}(0) \cdot \mathbf{S}(0) \rangle} = \alpha_0 e^{-t/\tau_1} + (1 - \alpha_0) e^{-t/\tau_2}, \quad (9)$$

where τ_1 is the short range characteristic timescale, τ_2 is the long range characteristic timescale, and α_0 ($0 \leq \alpha_0 \leq 1$) is a fitting parameter.

Figure 3(a) shows the temperature dependence of τ_1 and τ_2 . The slow decay characteristic timescale τ_1 decreases up to the transition temperature and then begins to increase, while τ_2 decreases monotonically. While τ_1 shows no clear monotonic trend with T , τ_2 demonstrates a temperature-dependent pattern that is qualitatively analogous to the behavior of κ . A power-law fit yields $\tau_2 \sim T^{-2.04}$ at lower temperatures below T_c , closely mirroring the thermal conductivity behavior, and $\tau_2 \sim T^{-0.57}$ at higher temperatures above T_c . In Figure 3(b), thermal conductivity is plotted against τ_2 , showing a clear linear relationship that directly links the long-scale characteristic time to thermal transport. This strong correlation supports the central role of τ_2 in governing the temperature-dependent thermal conductivity. While the double-exponential model elucidates the connection between thermal conductivity and HCACF decay, mode-dependent phonon analysis is required for a more comprehensive understanding.

To explore further the thermal transport mechanisms in monolayer germanene, we analyze the phonon density of states (DOS) and dispersion along the $\Gamma \rightarrow K \rightarrow M \rightarrow \Gamma$ path (Fig. 4(a)). The maximum LO/TO frequency of 14.1 THz aligns with Jiang et al. [22], and the absence of negative frequencies supports structural stability at simulated temperatures. As expected for 2D materials, the ZA mode exhibits quadratic dispersion, while TA and LA modes show cubic behavior [30, 31]. The DOS peak at 13.13 THz, dominated by LO phonons, undergoes a redshift with temperature, consistent with similar trends observed in other 2D materials [24, 25].

To assess temperature effects on phonon dispersion, we plot frequency deviations at high-symmetry points in Fig. 4(b-d). At Γ (Fig. 4(b)), acoustic modes remain unchanged due to symmetry, though the ZO mode shows significant redshift, reducing the acoustic-optical (AO) gap. Both TO and LO frequencies decrease modestly with temperature up to 650 K, after which redshifting intensifies. At the M point (Fig. 4(c)), the ZA and TA modes experience abrupt decrease in frequency around the transition temperature (350 K), with the TA mode exhibiting particularly strong redshifting. While ZO modes show frequency reductions across temperatures, minimal shifts in LA modes further compress the AO gap. At the K point, (Fig. 4(d)) the ZA modes show

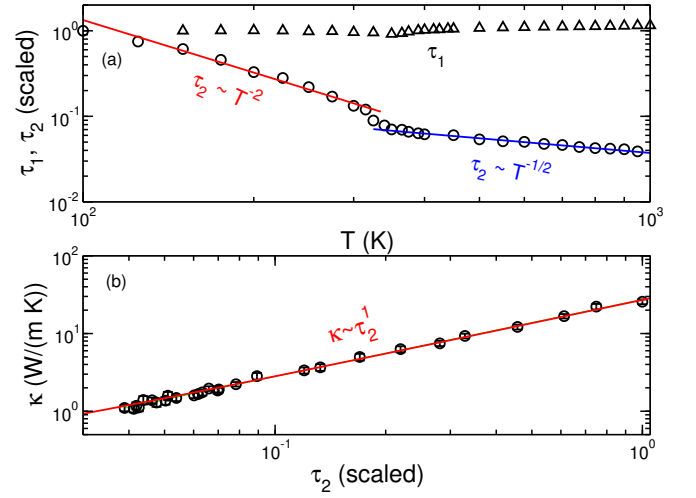


FIG. 3. (a) Scaled long-scale (circles) and short-scale (triangles) characteristic times with temperature for germanene monolayer, derived from double-exponential HCACF fitting, and (b) thermal conductivity as a function of the long-scale characteristic time. The long-scale characteristic time follows the same temperature dependence as thermal conductivity, while the short-scale characteristic time dips near the transition temperature.

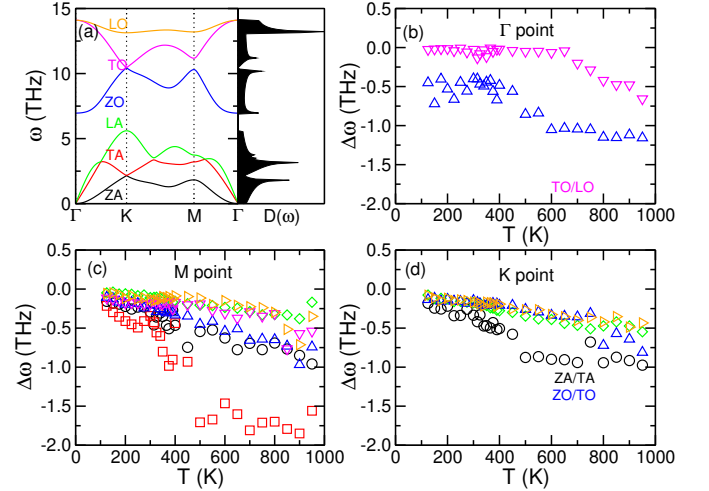


FIG. 4. (a) Phonon dispersion and density of states for germanene along $\Gamma \rightarrow K \rightarrow M \rightarrow \Gamma$ direction. (b-d) Angular frequency deviation from harmonic approximation with temperature at high-symmetry Γ , M, and K points. Notably, the acoustic gap narrows with temperature, contributing to thermal conductivity reduction.

significant redshifting near the transition temperature, while the ZO/TO and LA modes are slightly decreased, leading to a decreased AO gap. Overall, the AO gap narrowing with temperature significantly impacts thermal conductivity, similar to the observations in other 2D materials [32, 33]. The sharp AO gap reduction at M point likely correlates with the anomalous thermal conductivity transition.

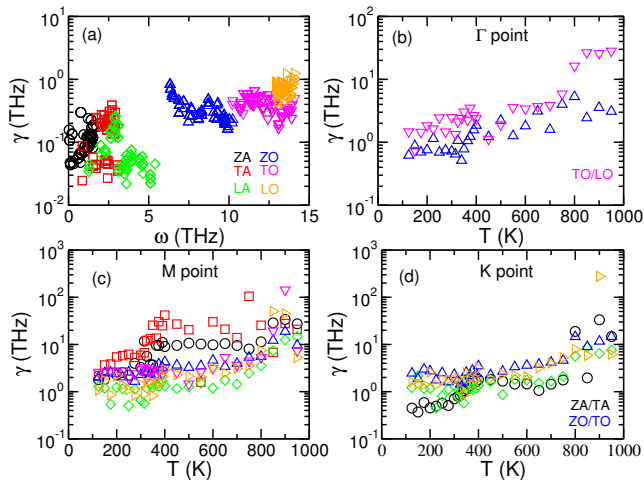


FIG. 5. (a) Mode-specific phonon linewidth of germanene at room temperature as a function of angular frequency. Phonon linewidth variation with temperature at (b) Γ , (c) M, and (d) K points. Linewidth increases with temperature, reducing phonon lifetimes and thermal conductivity.

In Fig. 5(a), we present the linewidth of different phonon branches with phonon angular frequency at the room temperature. The acoustic branches, primarily responsible for thermal transport are found to possess linewidths than optical modes. Intriguingly, unlike planar 2D materials like graphene, where the ZA mode displays suppressed linewidth, the out-of-plane and in-plane acoustic modes in germanene exhibit comparable linewidths at 300 K. The temperature-dependent phonon linewidths are plotted for Γ , M, and K points in Fig. 5(b-d). Linewidths increase with temperature, reflecting intensified phonon scattering at elevated temperatures. At Γ , optical phonon linewidths, particularly ZO, rise sharply near 350 K (Fig. 5(b)). The acoustic modes show significant increase in linewidth at the M point. From Fig. 5(c), it is evident that the linewidth of ZA and TA increase significantly at this symmetry point. Moreover, a clear transition is observed for TA and ZA phonons near the transition temperature. This rapid increase in linewidth reduces the phonon lifetime, thus reducing the thermal conductivity significantly. Similarly, at the K point the ZA/TA acoustic modes show rapid increase in linewidth near 350 K (Fig. 5(d)). This pronounced followed by a steady increase of acoustic phonon linewidths underpin the observed thermal conductivity transition.

D. Effect of Sample Size on κ

In low-dimensional materials, thermal conductivity often exhibits a pronounced dependence on sample dimensions, challenging the assumption of intrinsic behavior. In such cases, it is important to investigate the effect of sample length on the thermal transport in these materi-

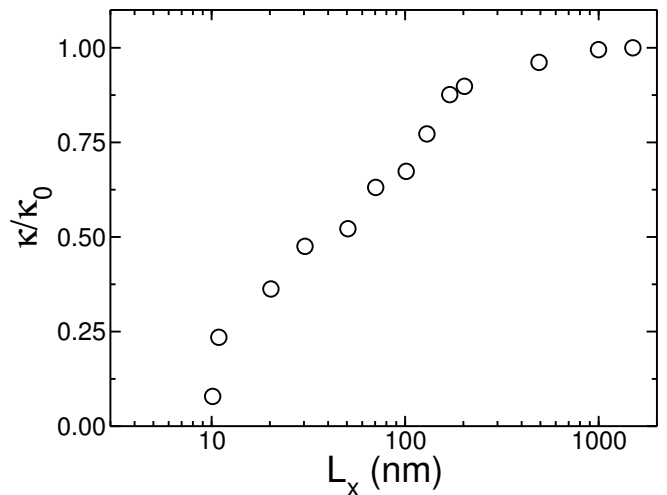


FIG. 6. Thermal conductivity of a germanene monolayer as a function of sample length, calculated using NEMD simulations at room temperature and scaled to thermal conductivity at a $1 \mu\text{m}$ sample length. A convergence in thermal conductivity is observed due to pronounced out-of-plane scattering.

als. Non equilibrium based approach is suitable for understanding the length dependence of thermal conductivity as the approach can simulate a microdevice measurement on sample placed in between hot and cold regions (Fig. S4 in SI) [34].

In Fig. 6, we present the thermal conductivity of monolayer germanene as a function of sample length, calculated at 300 K. Thermal conductivity increases consistently with length up to 500 nm before saturating at approximately $1 \mu\text{m}$. According to mode coupling theory, the behavior of the HCACF can indicate convergence or divergence in thermal conductivity, with t^{-1} scaling signifying divergence and $t^{-1.5}$ or faster indicating convergence [35]. Here, the scaled HCACF exhibits a decay of $t^{-1.6}$ (Fig. S5 in SI), indicating convergent thermal conductivity.

This convergence is attributed to the reduced contribution from flexural phonons, influenced by germanene's inherent buckling. Fig. 5(a) shows that the out-of-plane and in-plane acoustic phonon branches exhibit similar linewidths due to symmetry breaking caused by buckling. Consequently, the ZA phonons contribute less to the overall thermal conductivity, leading to convergence at larger sample sizes.

IV. CONCLUSIONS

In conclusion, we have systematically investigated the thermal conductivity mechanism of monolayer germanene using molecular dynamics simulations within the Green-Kubo formalism across an extensive temperature range, employing an optimized Stillinger-Weber potential parameter set. We report an anomalous temperature-

induced transition in the thermal conductivity of germanene monolayer at a critical temperature of 350 K. Our analysis reveal that the thermal conductivity follows an unusual scaling: $\kappa \sim T^{-2}$ below T_c , transitioning to $\kappa \sim T^{-1/2}$ above T_c , a stark departure from the typical $\kappa \sim T^{-1}$ trend. This anomalous scaling is closely mirrored in the slow relaxation timescale τ_2 of the HCACF, with $\tau_2 \sim T^{-2}$ below T_c and $\tau_2 \sim T^{-1/2}$ above, confirming the direct relationship $\kappa \sim \tau_2$.

Phonon analysis further elucidates this behavior, with a significant reduction in the AO gap, primarily due to redshifting of the TA phonon modes at high-symmetry M and K points. This redshifting, coupled with a rapid in-

crease in linewidths near T_c , signifies intensified phonon scattering, fundamentally altering the thermal transport pathways. Additionally, NEMD simulations indicate that the thermal conductivity of germanene converges with sample length, a characteristic attributed to comparable contributions from both in-plane and out-of-plane phonon modes, consistent with mode-coupling theory.

ACKNOWLEDGMENTS

The authors acknowledge Computer Center of IIT Jodhpur for providing computing resources that contributed to the research results reported in this paper.

-
- [1] J. Yuhara and G. L. Lay, Beyond silicene: synthesis of germanene, stanene and plumbene, *Japanese Journal of Applied Physics* **59**, SN0801 (2020).
- [2] A. Acun, L. Zhang, P. Bampoulis, M. Farmanbar, A. van Houselt, A. N. Rudenko, M. Lingenfelder, G. Brocks, B. Poelsema, M. I. Katsnelson, and H. J. W. Zandvliet, Germanene: the germanium analogue of graphene, *Journal of Physics: Condensed Matter* **27**, 443002 (2015).
- [3] N. J. Roome and J. D. Carey, Beyond graphene: Stable elemental monolayers of silicene and germanene, *ACS Applied Materials & Interfaces* **6**, 7743 (2014), pMID: 24724967, <https://doi.org/10.1021/am501022x>.
- [4] S. Cahangirov, M. Topsakal, E. Aktürk, H. Şahin, and S. Ciraci, Two- and one-dimensional honeycomb structures of silicon and germanium, *Phys. Rev. Lett.* **102**, 236804 (2009).
- [5] T. Arjmand, M. B. Tagani, and H. R. Soleimani, Buckling-dependent switching behaviours in shifted bilayer germanene nanoribbons: A computational study, *Superlattices and Microstructures* **113**, 657 (2018).
- [6] W. Li and N. Mingo, Thermal conductivity of fully filled skutterudites: Role of the filler, *Phys. Rev. B* **89**, 184304 (2014).
- [7] R. Chegel and S. Behzad, Tunable electronic, optical, and thermal properties of two-dimensional germanene via an external electric field, *Scientific Reports* **10**, 704 (2020).
- [8] M. Ye, R. Quhe, J. Zheng, Z. Ni, Y. Wang, Y. Yuan, G. Tse, J. Shi, Z. Gao, and J. Lu, Tunable band gap in germanene by surface adsorption, *Physica E: Low-dimensional Systems and Nanostructures* **59**, 60 (2014).
- [9] B. Mortazavi, A. Dianat, G. Cuniberti, and T. Rabczuk, Application of silicene, germanene and stanene for na or li ion storage: A theoretical investigation, *Electrochimica Acta* **213**, 865 (2016).
- [10] J. E. Padilha and R. B. Pontes, Electronic and transport properties of structural defects in monolayer germanene: An ab initio investigation, *Solid State Communications* **225**, 38 (2016).
- [11] C. Si, J. Liu, Y. Xu, J. Wu, B.-L. Gu, and W. Duan, Functionalized germanene as a prototype of large-gap two-dimensional topological insulators, *Phys. Rev. B* **89**, 115429 (2014).
- [12] B. Peng, H. Zhang, H. Shao, Y. Xu, G. Ni, R. Zhang, and H. Zhu, Phonon transport properties of two-dimensional group-iv materials from ab initio calculations, *Phys. Rev. B* **94**, 245420 (2016).
- [13] G. P. Das, P. R. Raghuvanshi, and A. Bhattacharya, Phonons and lattice thermal conductivities of graphene family, *Procedia Structural Integrity* **23**, 334 (2019), 9th International Conference Materials Structure & Micromechanics of Fracture (MSMF9).
- [14] Y. Tang, J. Che, and G. Qin, On the microscopic view of the low thermal conductivity of buckling two-dimensional materials from molecular dynamics, *Chemical Physics Letters* **780**, 138954 (2021).
- [15] Y. D. Kuang, L. Lindsay, S. Q. Shi, and G. P. Zheng, Tensile strains give rise to strong size effects for thermal conductivities of silicene, germanene and stanene, *Nanoscale* **8**, 3760 (2016).
- [16] X. Wang, Y. Hong, P. K. L. Chan, and J. Zhang, Phonon thermal transport in silicene-germanene superlattice: a molecular dynamics study, *Nanotechnology* **28**, 255403 (2017).
- [17] S. Jomehpour Zaveh, M. Roknabadi, T. Morshedloo, and M. Modarresi, Electronic and thermal properties of germanene and stanene by first-principles calculations, *Superlattices and Microstructures* **91**, 383 (2016).
- [18] D. L. Nika and A. A. Balandin, Phonons and thermal transport in graphene and graphene-based materials, *Reports on Progress in Physics* **80**, 036502 (2017).
- [19] A. A. Balandin, S. Ghosh, W. Bao, I. Calizo, D. Teweldebrhan, F. Miao, and C. N. Lau, Superior thermal conductivity of single-layer graphene, *Nano Letters* **8**, 902 (2008), pMID: 18284217, <https://doi.org/10.1021/nl0731872>.
- [20] L. Lindsay, W. Li, J. Carrete, N. Mingo, D. Broido, and T. Reinecke, Phonon thermal transport in strained and unstrained graphene from first principles, *Physical Review B* **89**, 155426 (2014).
- [21] A. P. Thompson, H. M. Aktulga, R. Berger, D. S. Bolintineanu, W. M. Brown, P. S. Crozier, P. J. in 't Veld, A. Kohlmeyer, S. G. Moore, T. D. Nguyen, R. Shan, M. J. Stevens, J. Tranchida, C. Trott, and S. J. Plimpton, LAMMPS - a flexible simulation tool for particle-based materials modeling at the atomic, meso, and continuum scales, *Comp. Phys. Comm.* **271**, 108171 (2022).
- [22] J.-W. Jiang and Y.-P. Zhou, *Handbook of Stillinger-Weber Potential Parameters for Two-Dimensional*

Atomic Crystals (IntechOpen, Rijeka, 2017).

- [23] S. Thapliyal, S. S. Paul Chowdhury, and S. Mogurampelly, Modeling germanene monolayer: Interaction potentials and insights into the phonon thermal conductivity, in *Energy Materials and Devices*, edited by A. Dixit, V. K. Singh, and S. Ahmad (Springer Nature Singapore, Singapore, 2024) pp. 325–335.
- [24] H. Chakraborty, S. Mogurampelly, V. K. Yadav, U. V. Waghmare, and M. L. Klein, Phonons and thermal conducting properties of borocarbonitride (bcn) nanosheets, *Nanoscale* **10**, 22148 (2018).
- [25] S. S. Paul Chowdhury, A. Samudrala, and S. Mogurampelly, Modeling interlayer interactions and phonon thermal transport in silicene bilayers, *Phys. Rev. B* **108**, 155436 (2023).
- [26] A. Carreras, A. Togo, and I. Tanaka, Dynaphopy: A code for extracting phonon quasiparticles from molecular dynamics simulations, *Computer Physics Communications* **221**, 221 (2017).
- [27] J. Yuhara, D. Matsuba, M. Ono, A. Ohta, S. Miyazaki, M. Araidai, S. ichi Takakura, M. Nakatake, and G. Le Lay, Formation of germanene with free-standing lattice constant, *Surface Science* **738**, 122382 (2023).
- [28] G. Qin, Z. Qin, H. Wang, and M. Hu, Anomalously temperature-dependent thermal conductivity of monolayer gan with large deviations from the traditional $1/t$ law, *Phys. Rev. B* **95**, 195416 (2017).
- [29] P. Carruthers, Theory of thermal conductivity of solids at low temperatures, *Rev. Mod. Phys.* **33**, 92 (1961).
- [30] S. S. Paul Chowdhury and S. Mogurampelly, Unusual phonon thermal transport mechanisms in monolayer beryllene (2024), arXiv:2409.05766 [cond-mat.mtrl-sci].
- [31] X. Gu and R. Yang, First-principles prediction of phononic thermal conductivity of silicene: A comparison with graphene, *Journal of Applied Physics* **117**, 025102 (2015), https://pubs.aip.org/aip/jap/article-pdf/doi/10.1063/1.4905540/15157174/025102_1_online.pdf.
- [32] L. Lindsay, D. A. Broido, and T. L. Reinecke, First-principles determination of ultrahigh thermal conductivity of boron arsenide: A competitor for diamond?, *Phys. Rev. Lett.* **111**, 025901 (2013).
- [33] X. Gu and R. Yang, Phonon transport in single-layer transition metal dichalcogenides: A first-principles study, *Applied Physics Letters* **105**, 131903 (2014), https://pubs.aip.org/aip/apl/article-pdf/doi/10.1063/1.4896685/8608036/131903_1_online.pdf.
- [34] X. Gu, Y. Wei, X. Yin, B. Li, and R. Yang, Colloquium: Phononic thermal properties of two-dimensional materials, *Rev. Mod. Phys.* **90**, 041002 (2018).
- [35] S. Lepri, R. Livi, and A. Politi, Thermal conduction in classical low-dimensional lattices, *Physics Reports* **377**, 1 (2003).